International Journal of Computer Assisted Radiology and Surgery (2019) 14:1227–1235
https://doi.org/10.1007/s11548-019-01998-y

ORIGINAL ARTICLE

Dynamic, patient-specific mitral valve modelling for planning transcatheter repairs

Olivia K. Ginty[1] · John T. Moore[1] · Mehdi Eskandari[2] · Patrick Carnahan[1] · Andras Lasso[3] · Matthew A. Jolley[4] · Mark Monaghan[2] · Terry M. Peters[1,5]

Received: 12 March 2019 / Accepted: 14 May 2019 / Published online: 21 May 2019

Abstract

***Purpose*:** Transcatheter, beating heart repair techniques for mitral valve regurgitation is a very active area of development. However, it is difficult to both simulate and predict the clinical outcomes of mitral repairs, owing to the complexity of mitral valve geometry and the influence of hemodynamics. We aim to produce a workflow for manufacturing dynamic patient-specific models to simulate the mitral valve for transcatheter repair applications.

***Methods*:** In this paper, we present technology and associated workflow, for using transesophageal echocardiography to generate dynamic physical replicas of patient valves. We validate our workflow using six patient datasets representing patients with unique or particularly challenging pathologies as selected by a cardiologist. The dynamic component of the models and their resultant potential as procedure planning tools is due to a dynamic pulse duplicator that permits the evaluation of the valve models experiencing realistic hemodynamics.

***Results*:** Early results indicate the workflow has excellent anatomical accuracy and the ability to replicate regurgitation pathologies, as shown by colour Doppler ultrasound and anatomical measurements comparing patients and models. Analysis of all measurements successfully resulted in $t\ critical\ two\text{-}tail > t\ stat$ and p values > 0.05, thus demonstrating no statistical difference between the patients and models, owing to high fidelity morphological replication.

***Conclusions*:** Due to the combination of a dynamic environment and patient-specific modelling, this workflow demonstrates a promising technology for simulating the complete morphology of mitral valves undergoing transcatheter repairs.

Keywords Modelling · Mitral valve · Mitral valve models · Surgical simulation · Transcatheter devices · 3D printing

Introduction

Mitral valve regurgitation (MR) is the most common heart valve condition, affecting 2.5% of the general population, with prevalence increasing to over 9% for those aged 75 and older [1]. However, 50% of patients with severe mitral valve disease are not candidates for surgery due to their age or co-morbidities [2]. Furthermore, increased MR severity is associated with increased mortality [3]. In recent years numerous beating heart, transcatheter devices have been developed to try and replicate (or replace) mitral valve repair techniques in an effort to assist this population.

The mitral valve (MV) apparatus is a complex, dynamic structure consisting of anterior and posterior valve leaflets, annulus, and chordae tendinae that connect the leaflets to papillary muscles, which are in turn part of the left ventricle. The saddle-shaped annulus anchors the MV between the left atrium and ventricle and the apparatus collectively prevents the backflow of blood during the contraction of the left ventricle, thus serving a vital role in ensuring efficient cardiac output. MR is defined by leaking of the MV as it fails in its role to prevent backflow. A wide variety of conditions

✉ Olivia K. Ginty
oginty@uwo.ca

1 Robarts Research Institute, Western University, London N6A5B7, Canada

2 King's College Hospital, Denmark Hill, London SE59RS, UK

3 Laboratory for Percutaneous Surgery, Queen's University, Kingston K7L3N6, Canada

4 Department of Anesthesiology and Critical Care Medicine/Division of Pediatric Cardiology, Children's Hospital of Philadelphia, University of Pennsylvania Perelman School of Medicine, Philadelphia 19104, USA

5 Department of Medical Biophysics, Medical Imaging, School of Biomedical Engineering, Western University, London N6A3K7, Canada

can cause MR, either directly as an alteration of the MV apparatus (degenerative MR disease), or as a secondary consequence to alterations in the left ventricle (functional MR). Transcatheter repairs typically attempt to replicate various surgical techniques for treating MR. The MitraClip (Abbott Laboratories, Abbott Park, IL, USA), for example, replicates the edge-to-edge surgical technique by clipping the edges of the two-valve leaflets together, while the Cardioband (Edwards Life Sciences) replicates surgical annuloplasty, where a ring is fitted into the valve annulus to reduce its overall size. Beyond these, as of 2018 there are eight devices being studied in humans for mitral annuloplasty, five in clinical trials for repairing or replacing chordae tendinae, and more than ten transcatheter mitral valve replacement devices at various stages of development and clinical trials [4]. The first of these devices to be used in humans was the MitraClip in 2003 and since then, more than 35,000 MitraClip procedures have been performed worldwide primarily for functional MR [5]. In contrast, the total number of transcatheter aortic valve replacements (TAVR) is expected to reach $>$ 125,000 in 2018 alone [6]. This discrepancy is largely due to the relative complexity of the MV apparatus, in comparison with the aortic valve [7].

Evaluating the safety and efficacy of new devices is challenging, as animal trials, while invaluable, are costly and time-consuming, making them better suited to more established devices. Dynamic, ex vivo heart devices have been developed, offering views inside newly excised animal and even human hearts [8,9]. These simulators have been used to observe valves functioning in a saline solution, providing highly valuable information with direct vision and real biological tissues. However, the simulators are arduous and costly to prepare, and the mitral valves themselves are neither pathologic nor patient-specific.

Device development faces challenges beyond assessing their safe use in patients, as the additional selection of the most suitable approach for a specific patient can be difficult. As the number of repairs already performed climbs, guidelines for MitraClip use are becoming clearer. Yet, a substantial grey area still remains, where it is unclear whether MV surgery, transcatheter repair, or ongoing medical therapy is the best option for specific patients. Thus, the weighing of approaches and their associated disadvantages or potential futility persists as one of the largest clinical tribulations for devices such as the MitraClip [10]. Given the complexity of MV morphology, hemodynamics, and variety of pathologies, the process of choosing both the appropriate device and its manner of implementation can be challenging. As a result, there is a demand for high fidelity valve models capable of replicating the complexity of mitral valve disease and dysfunction. However, this is a challenge as it requires the mitral valve simulator and phantoms to replicate multiple tissue properties, the specifics of which depend on the application, and on the available technology. For example, a generic realistic tissue-mimicking polyvinyl alcohol MV can be provided as a basic repair training tool, without patient specificity or hemodynamics [11]. In another cases, flexible 3D-printed materials have been used to replicate patient-specific MV's to study precise mitral anatomy or simulate an intervention without replication of realistic hemodynamics [12,13]. 3D printing has also been used indirectly to produce moulds for patient-specific tissue-mimicking silicone for simulating on-pump minimally invasive MV repairs, in a non-hemodynamic environment [14]. In other models, researchers have replicated a hemodynamic environment for use with excised bovine MVs, to provide data for mathematical modelling [15]. However, to the best of our knowledge no previous work has combined all three of hemodynamic environment, functional repairable valves, and patient-specific modelling [16].

In our previous work, we presented a valve simulator and workflow for creating patient-specific silicone-based valve models [17]. However, this work was limited by a simulator that was incapable of completely mimicking human hemodynamics. The ability to physically model a patient's valve and replicate the dynamic valve behaviour in a hemodynamically realistic environment offers a powerful evaluation tool to clinicians assessing different repair options. It also offers benchtop and device researchers a controlled and easily replicated environment, for rapidly improving and validating new cardiac-associated technologies. To that end, our goal in this paper is to use a new pulse duplicator capable of replicating the MV in a realistic environment with higher fidelity, to simulate the valves of six Mitraclip patients and validate the replicas using 2D and 3D Doppler ultrasound. The new device, called the Mitral Valve Simulator (MVS) pulse duplicator, is capable of accurately replicating realistic human MV pressure gradients, left ventricle stroke volume, and heart rates.

This system was designed to seamlessly integrate into the treatment protocol of a typical MR patient, as diagnostic 3D transesophageal echocardiography (TEE) images can be used to create a geometric model of the patient's MV. This model can then be segmented and 3D printed using an inexpensive fused deposition modelling printer, permitting one or more valve replicas to be created within two days following TEE data acquisition. The replicas can then be loaded into the pulse duplicator, and their artificial chordae tendinae can be interactively adjusted to best mimic the patient pathology. Clips can then be applied to the valve, with Doppler ultrasound and visual inspection applied to help identify the optimal number and location of clips. It is feasible to complete this process between the day of diagnostic TEE and the day of intervention. In the following section, we first briefly outline the method for creating physical replicas along with our segmentation software. We then summarize the new

pulse duplicator and its operation. Finally, we describe the patient data, the respective replicated dynamic models, and our assessment of the replication accuracy.

Methods

In this section, we outline the three main steps necessary to create patient-specific valve replicas. The TEE image data must be segmented and the resultant valve profiles 3D printed, to permit the manufacture of dynamic tissue-mimicking replicas, which are then tested in the pulse duplicator. We summarize these steps below, followed by an outline of our validation strategy.

MV segmentation

Our segmentation software is based on the open-source platform 3D Slicer [18], and the Insight Segmentation and Registration Toolkit (ITK) [19]. The segmentation software implements an interactive-automatic approach with limited user input required to complete a segmentation. Before performing the segmentation, the user must select the image frame before systole where the leaflets are not yet coapted. This cardiac phase minimizes issues with ultrasound signal dropout while still showing two clearly distinct leaflets. The user then defines the annulus contour and the papillary tip locations using the SlicerHeart module [20]. Our segmentation algorithm then begins by performing a segmentation of the blood pool using a geodesic active contour approach [21] which is biased to grow. The completed blood pool segmentation is then used to define a region of interest which initializes the leaflet segmentation (Fig. 1a). A second active contour segmentation, biased to shrink, is applied to the leaflets until the user is satisfied with the results. Because the contour segmentation steps require the user to run the automatic segmentation algorithm in increments until the segmentation is judged to be complete, our algorithm uses an interactive-automatic approach. This interactive approach is proved to be more effective than a fully automatic approach, as choosing a fixed stopping point led to inconsistent results since there is inherent variability in the ultrasound images taken from different patients. The details and validation of this segmentation will be examined more deeply in a separate paper, recently accepted for publication [22]. However, preliminary results from performing both algorithm-based and manual segmentations on nine different patient datasets revealed promising accuracy between the extracted proximal surfaces of the segmentations, with a mean absolute surface distance of $1.01\,\text{mm} \pm 0.74\,\text{mm}$.

In addition to defining the surface geometry for the MV apparatus, our application requires translating this information into a polydata format capable of being 3D printed and integrated into our pulse duplicator. To this end, the leaflet surface that is proximal to the TEE source is isolated, and normals for its polydata surface are inverted to create a model of the *en face* view of the valve, including as much of the LA wall as possible based on the TEE field of view. This new polydata surface is then cropped with a base that matches the 3D printed valve flange, as described in Fig. 1.

Replicating valves in silicone

The workflow for creating valve replicas is described in detail in our previous work [17]. In summary, the segmented surface of the patient MV is 3D printed and fitted into a tray in which silicone is poured (Fig. 2a, b). Gauze fabric is cut to the shapes of the anterior and posterior leaflets, infused with silicone and then painted onto the 3D printed valve profile (Fig. 2c). Without gauze, silicone lacks the tensile strength of the leaflets, and sutures or clips would easily dehisce under the load of normal human hemodynamic pressures. In addition to gauze, a braided nylon thread is frayed and embedded into the silicone to replicate a total of six chordae tendinae, which further divide, imitating the human anatomical equivalents (Fig. 2d). Braided nylon adequately mimics both the flexibility of the chordae, as well as the strength required to operate under realistic hemodynamics. The silicone, chordae strings and gauze all cure together on a rotation device, which rotates the valve ensuring it settles evenly (Fig. 2a) before additional silicone is applied to create a surrounding flange (Fig. 2e). Using Spaceclaim CAD software (ANSYS Inc., Canonburg, USA), the posts for the papillary muscles are tailored to accurately represent the location of the papillary tips as defined in SlicerHeart using the patients TEE ultrasound data. These papillary posts are 3D printed and fitted to the flange assembly for the MV (Figs. 2f, 3b). The two posts each incorporate three shafts that allow for individually adjusting a total of six separate chordae tendinae, as described below.

Mitral valve simulator (MVS) pulse duplicator

The overall design of the MVS device is intended to provide a high fidelity representation of the in vivo, dynamic MV environment that is also inexpensive and easy to operate. Full details and validation of the pulse duplicator system are published elsewhere [23]. In brief, it is comprised of a motor assembly and diaphragm for mimicking the contractile left ventricle, a two chambered box, and an aortic outflow tower (Fig. 4a). The valve assembly mounts inside the high pressure chamber. An opening in the valve assembly connects directly to an aortic outflow tube with a ball valve and spring (Fig. 4b), which provide a resisting force to approximate LV afterload pressures. Adjusting the tension on the spring changes the systolic pressure. The spring structure is housed

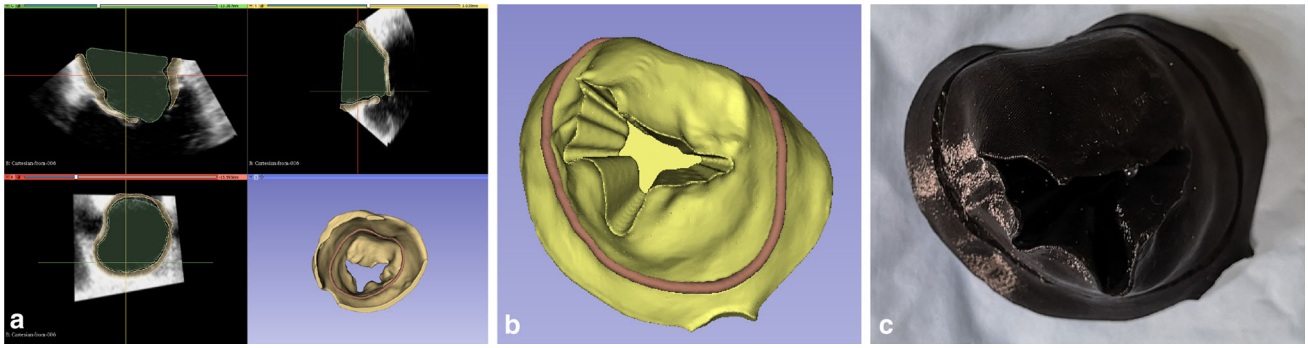

Fig. 1 **a** TEE image data and segmentation in Slicer: Leaflet segmentation (yellow) initialized from outer region of blood pool segmentation (green); **b** segmented model of valve surface proximal to TEE probe; **c** 3D printed replica of the proximal valve surface. The mitral valve annulus is included to help modelling the left atrial and ventricle boundary

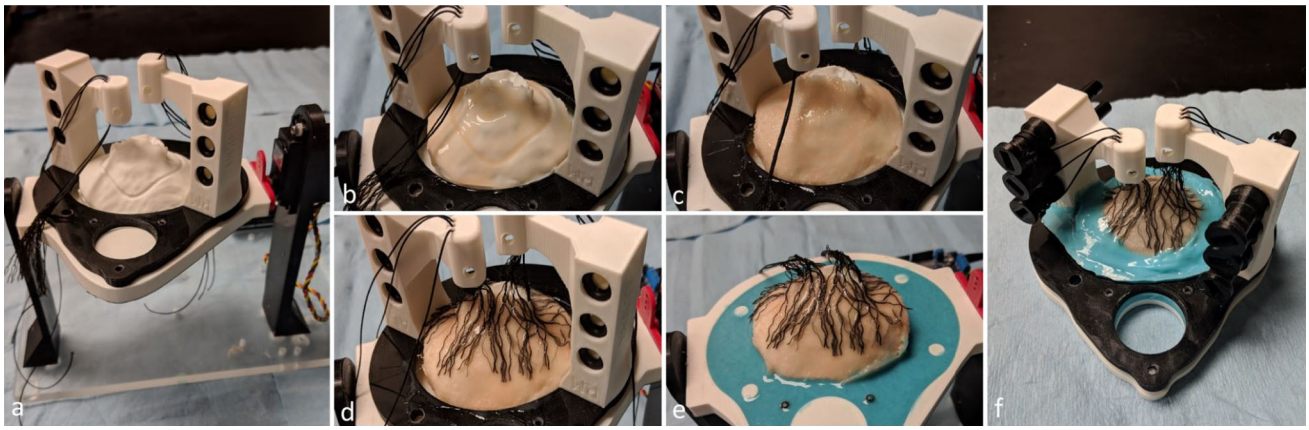

Fig. 2 **a** Patient-specific valve profile with annulus indentation and papillary muscles attached to rotation device; **b** application of tissue-mimicking silicone to valve profile; **c** gauze applied to valve; **d** chordae strings applied to valve; **e** additional silicone applied to surrounding flange mould; **f** final result with additional silicone reinforcing left atrium tissue proximal to annulus, and chordae strings secured to adjustment posts

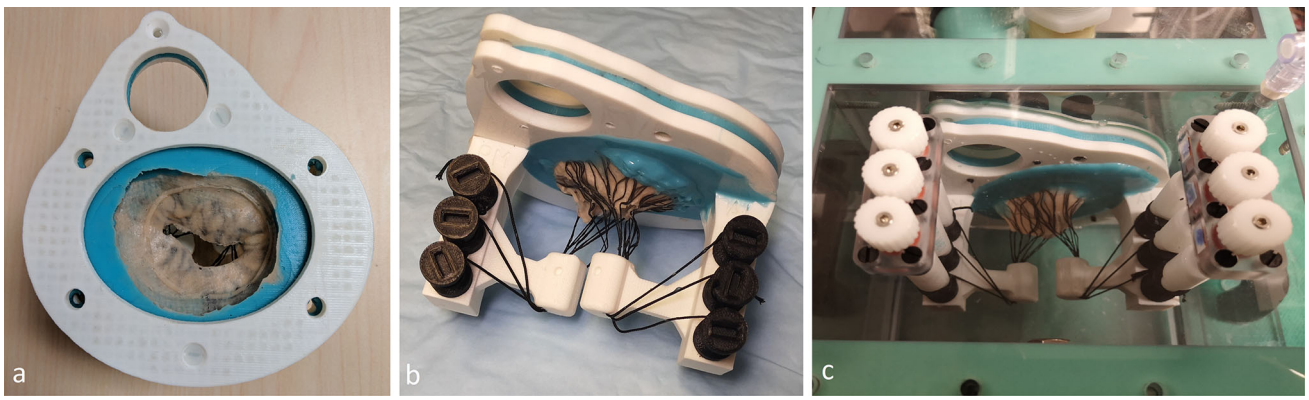

Fig. 3 **a** The *en face* view of the MV and flange; **b** the valve assembly with flange, papillary posts and adjustable chordae; **c** the valve assembly mounted in the MVS pulse duplicator. Dials on the lid of the device connect to the papillary posts so the chordae can be adjusted while the device is in operation

inside a larger tube that is open to the low pressure (atrial) chamber. The height of water or blood mimicking fluid in this outer tower mimics left atrial pressures. By adjusting the spring size and tension, the MVS can create systolic ventricular pressures of over 200 mmHg, while the atrial pressure is 10 mmHg when a competent valve in installed. For this

study, our systolic ventricular pressure was set to 105 mmHg in the presence of such a valve.

The lid of the device incorporates six columns which have individual external dials and align with the six posts to which chordae tendinae are attached (Fig. 3c). This makes it possible for the user to interactively adjust individual chordae lengths to best match patient pathology, as seen in TEE Doppler imaging, while the device is in operation. Alternatively, chordae lengths can be adjusted to evaluate the effect that lengths have on valve performance and hemodynamics.

Validation

The echocardiography data collection inclusion criteria accepted patients with severe mitral regurgitation, worked up for MitraClip therapy in a tertiary centre with expert level 3D TEE (Kings College Hospital, London, UK). These clinical datasets were de-identified and untraceable, and employed in this research in accordance with European General Data Protection Regulation (GDPR) standards, ethical standards of the institutional and/or national research committee and with the 1964 Helsinki Declaration and its later amendments or comparable ethical standards. For this type of retrospective image collection study, formal consent is not required. Six patient data sets were obtained, including 5 males and 1 female, an average patient age of 81 and no remarkable shared characteristics outside their valve disease. The cases included both degenerative and functional MR, of which five had undergone MitraClip intervention, and one had been deemed technically challenging and was subsequently referred for high-risk open-heart surgery. The data sets selected represent a mix of straightforward and technically challenging cases. All six were segmented, and valve profiles printed on an inexpensive 3D printer, Ultimaker 3 (Ultimaker, Geldermalsen, The Netherlands). The silicone replicas were loaded into the pulse duplicator, and TEE data collected. Both patient and replica data were acquired using the Philips Epiq system (Philips Ultrasound Inc. Reedsville, USA). An expert used Philips QLab software to quantify anatomical and pathology data for both datasets. The anatomical measurements included the anterolateral–posteromedial and anterior–posterior diameters, of the valves, as well as their annular circumference, 2D area, and 3D area (surface area when accounting for contour of annulus). Finally, annular ellipticity was a measurement to quantify the iconic saddle shape of the mitral valve. These measurements collectively summarized the anatomical accuracy, while functionality was reflected in the presentation of the regurgitation jet. Vena contracta width is a clinically used measurement for quantifying mitral regurgitation and was therefore measured across the patients and models to evaluate the replication of the regurgitation. It is obtained by measuring the width of the highest velocity region of the regurgitation jet, in the anterior–posterior axis.

Statistical analysis

In this study, mean and standard deviation (SD) expressed continuous variables, while percentages expressed categorical variables, and paired *t*-tests analysed dichotomous variables, with the two-tailed p value < 0.05 being considered statistically significant.

Results

Analysis with QLab anatomical quantification and regurgitation evaluation revealed promising correlation between the models and their patient valve counterparts. As given in Tables 1 and 2, five different anatomical measurements demonstrate the accuracy the models achieved in replicating each patients valve. Statistical analysis resulted in t *critical (two-tailed)* $> t$ *stat*, and p values all greater than 0.05 (anterolateral–posteromedial diameter p value $= 0.80$, posterior–anterior diameter p value $= 0.21$, annular 3D circumference p value $= 0.65$, annular 2D area p value $= 0.79$, annular 3D min area 0.42, annular ellipticity p value $= 0.84$). Thus, no statistical difference was found between the patients and models in these measurements, reflecting the similarity of the models to the patients across a multitude of dimensions. Additionally measurement and analysis of the vena contracta width across the valves, Table 3, also resulted in t *critical (two-tailed)* $> t$ *stat*, and p value greater than 0.05 (p value $= 0.12$), again suggesting that there was little difference between the patients and models. Patients 4 and 5 were excluded from measurements of vena contracta due to the inadequacy of their images for measuring these magnitudes. These measurements demonstrate the anatomical and regurgitation aspects of accuracy of the models, thus collectively summarize this workflows ability to adequately replicate patient morphologies.

In addition to these numerical results, we emphasize the more subjective, but nonetheless important simulation quality of these models. As shown by Fig. 4, the model and dynamic simulator permit a visually similar appearance both physically and under TEE imaging to that observed with actual patient mitral valves. This figure also provides a visual example of how each regurgitation jet location was matched with the patients regurgitation, as seen in 3D TEE with colour Doppler. The model TEE with colour shows additional regions of enhancement which we believe to be caused by small unassociated turbulences in the simulator, and the model TEE without colour shows an artefact of the white papillary posts visualized in the photograph of the model. Regardless of these artefacts, since transcatheter interven-

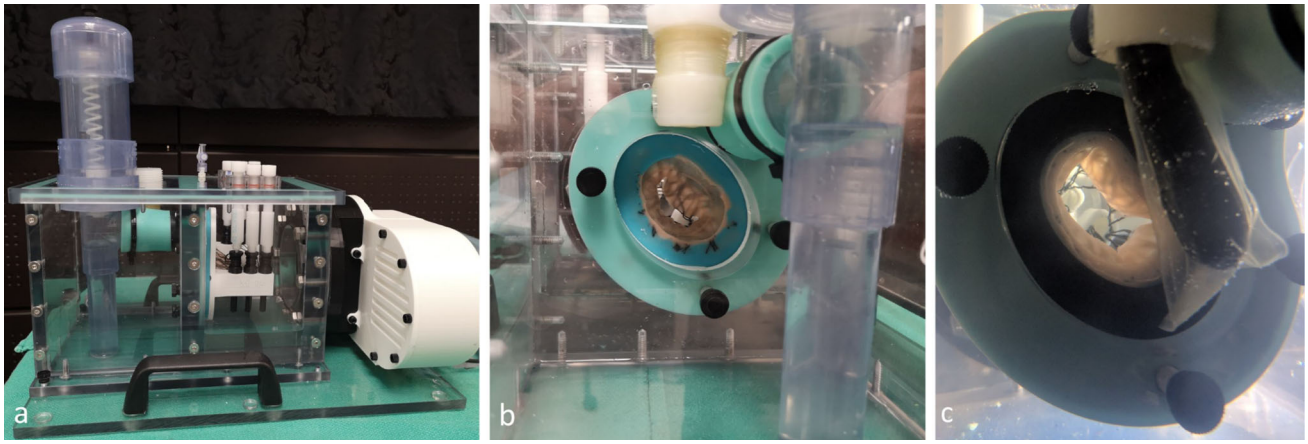

Fig. 4 The MVS pulse duplicator. **a** side view showing (from left) atrial reservoir/low pressure chamber with aortic outflow tower, left ventricle/high-pressure chamber with mounted valve assembly, and motor assembly; **b** end view with TEE access port (top centre), and valve in place; **c** closer end view with the TEE probe in place and chordae and papillary posts visible through the valve

Table 1 Anatomical measurements of Patient (P) and Model (M) mitral valves

Case	Anterolateral–posteromedial diameter (mm)		Anterior–posterior diameter (mm)		Annular 3D circumference (mm)		Annular 2D area (mm^2)		Annular 3D min area (mm^2)		Annular ellipticity (%)	
	P	M	P	M	P	M	P	M	P	M	P	M
1	37.2	35.6	40.6	40.9	129.2	137.7	1188.5	1218.6	1231	1344.6	92.9	89
2	40.6	41	44.2	42	140.3	146.9	1368.1	1468.4	1422.9	1526.3	92	97.2
3	41.9	49	41.8	38	138.4	142.6	1450.3	1423	1467.2	1458	100	124
4	37.1	34.3	31.5	32.6	118.3	125.8	939.1	1122	999.4	1165	117.7	105
5	43.2	40.7	47.4	34	147	132.5	N/A	N/A	N/A	N/A	N/A	N/A
6	39.4	36.3	35.6	34.7	126.7	124.8	1126.3	930	1172.8	1040	110.7	105
Mean	39.9	39.5	40.2	37.0	133.3	135.1	1214.5	1232.4	1258.7	1306.8	102.7	104.0
± SD	2.26	4.94	5.28	3.53	9.56	8.18	180.83	197.91	170.77	180.98	10.07	11.60

tions rely heavily on TEE guidance, the quality of the TEE of the model itself is noteworthy and suggests potential for future repair simulation applications (Fig. 5).

Discussion

The mitral valve apparatus is a complex structure, whose behaviour and dysfunction can only be properly understood when the valve is observed within a realistic hemodynamic environment. Simulation provides an opportunity to examine the ideal approach for a patient-specific MV morphology and condition. For procedures such as the MitraClip, it permits patient-specific planning to assess the ideal number of clips and location resulting in the least residual MR. Additionally, simulation provides a risk-free environment for training, and for testing different treatment options without the priority of patient safety. This paper examined the first steps in this process, validating the accuracy of the mitral valve and pathology in a simple but realistic hemodynamic environment. Our results successfully demonstrate the accuracy of the models with respect to multiple parameters of the MV physiology with no statistical difference found between the groups. MV function as defined by vena contracta width suggests our models can accurately mimic MV pathology.

Although we believe our research presents an innovative simulation tool, there are important limitations. By 3D printing a mould for the atrial surface of the mitral valve, we avoid the expense and limitations in material strength associated with direct 3D printing. This also permitted us to incorporate extensive chordae tendinae necessary to mimic leaflet motion and pathology, and a mesh to maintain the integrity of the model leaflets during repair. However, this technique results in leaflets that appear approximately 1 to 2 mm thicker than real MV leaflets under TEE imaging, due to the attenuation of silicone, making some imaging evaluations challenging such as regurgitation measurements. This at times limited our ability to obtain data in our study, as was mentioned with data

Table 2 Paired *t*-test analysis of anatomical measurements

Anatomical measurement	Paired *t*-test, two-tailed	*p* value
Anterolateral–posteromedial diameter (mm)	*t* critical two-tail > *t* stat	0.80
Anterior–posterior diameter (mm)	*t* critical two-tail > *t* stat	0.21
Annular 3D circumference (mm)	*t* critical two-tail > *t* stat	0.65
Annular 2D area (mm^2)	*t* critical two-tail > *t* stat	0.79
Annular 3D min area (mm^2)	*t* critical two-tail > *t* stat	0.42
Annular ellipticity (%)	*t* critical two-tail > t stat	0.84

Table 3 Regurgitation measurement and analysis

Case	Vena contracta width (mm)	
	Patient	Model
1	6.0	5.6
2	6.0	6.1
3	8.0	7.4
6	7.9	7.0
Mean	7.0	6.5
± SD	$9.78 \times 10^{-}2$	7.12×10^{-2}
Paired *t*-test, two-tailed	*t* critical two-tail > *t* stat	*p* value = 0.12

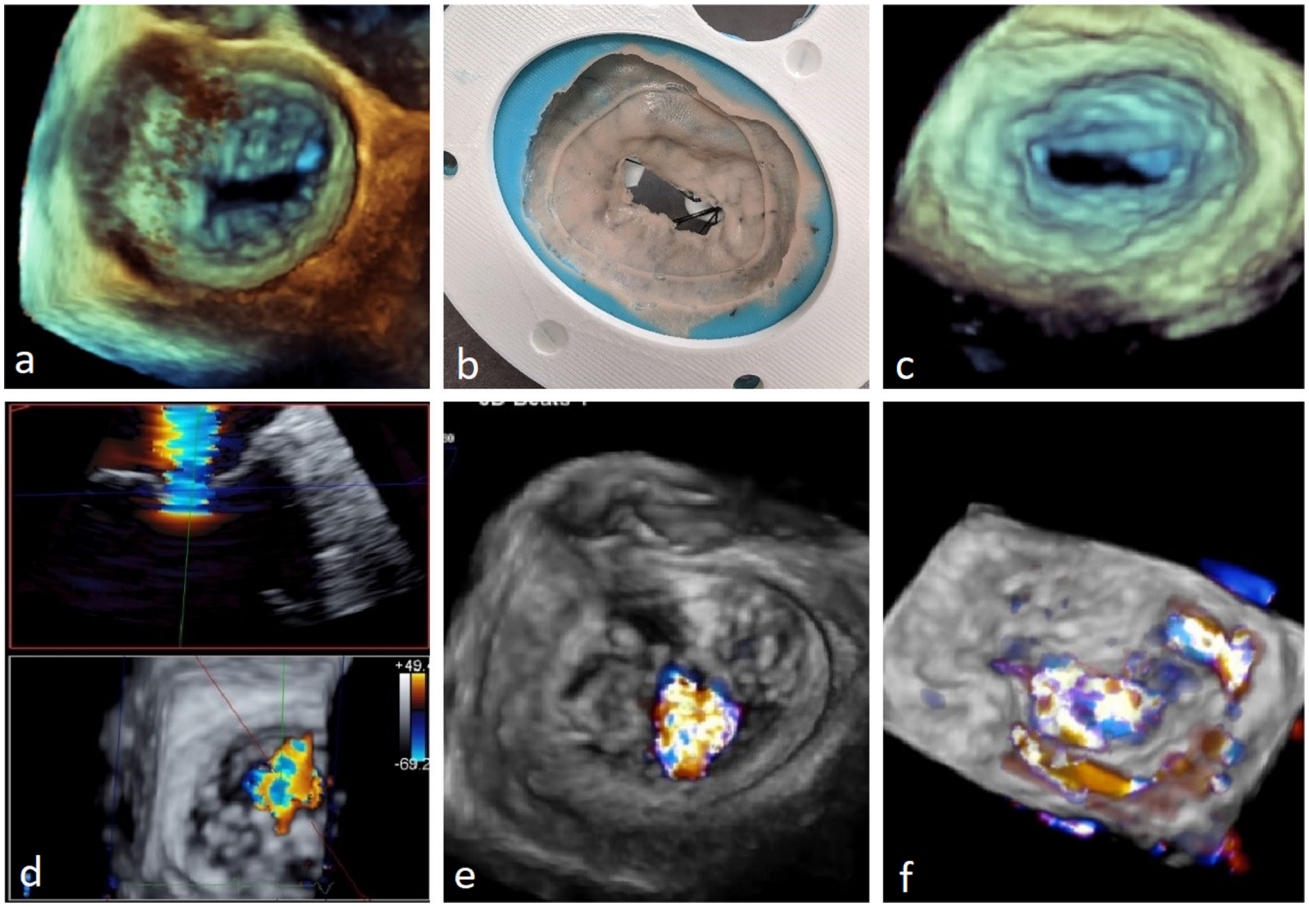

Fig. 5 **a** 3D TEE of Patient 2; **b** model of Patient 2; **c** 3D TEE of Patient 2 model; **d** Left, Screen capture of QLab analysis examining the vena contracta width; **e** 3D TEE with colour Doppler of Patient 2; **f** 3D TEE with colour Doppler of Model of Patient 2

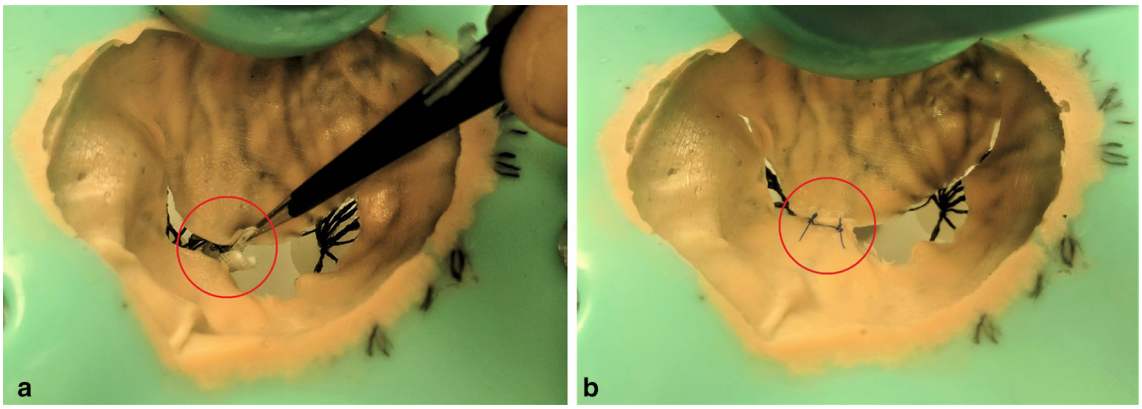

Fig. 6 **a** Model valve with sample non-deployed Mitraclip, encircled in red; **b** same model with edge-to-edge stitch in place of the Mitraclip, encircled in red

sets 4 and 5. Finally, our relatively small subject cohort limits the statistical validity of our results. Future work will include a larger sample size, as well as the validation of our ability to replicate actual patient repair results on our model valves. An example of this is shown in Fig. 6b, which demonstrates a simulated patient-specific Mitraclip repair, completed using a edge-to-edge stitch in same precise location as the patient's Mitraclip. This surgical stitch predates the Mitraclip system and shares the same mechanism for improving functionality, and in our future research study application, it serves as a substitute for the costly and rarely accessible Mitraclips (Fig. 6a).

Conclusion

We present a complete workflow for generating patient-specific mitral valve models based on diagnostic ultrasound data. We validate our workflow using six patient datasets from MitraClip cases. The valve models are segmented, then their *en face* profile is 3D printed, and finally silicone models are created. These models can then be loaded into a hemodynamically realistic mitral valve simulator device, and the valves can be assessed in a truly dynamic environment. The goal of this work is to provide researchers with a workflow for evaluating new MV repair technologies and also provides clinicians with a simulator with which they can assess patient-specific repair options prior to the actual intervention.

Acknowledgements The authors would like to thank Paul Picot and Kevin Barker for help in the design and construction of the MVS pulse duplicator, Nora Boone for help in its validation and Dave Ly for help in computer-aided design (CAD) software work. *Funding*: This study was funded by the Academic Medical Organization of Southwestern Ontario, as well as by the Canadian Foundation for Innovation (20994), the Ontario Research Fund (IDCD), and the Canadian Institutes for Health Research (FDN 201409).

Compliance with ethical standards

Conflict of interest John Moore and Terry Peters are co-owners of Archetype Medical, developers of the MVS pulse duplicator. The other authors declare no conflicts of interest.

References

1. Benjamin EJ, Virani SS, Callaway CW, Chamberlain AM, Chang AR, Cheng S, Chiuve SE, Cushman M, Delling FN, Deo R, De Ferranti SD, Ferguson JF, Fornage M, Gillespie C, Isasi CR, Jiménez MC, Jordan LC, Judd SE, Lackland D, Lichtman JH, Lisabeth L, Liu S, Longenecker CT, Lutsey PL, MacKey JS, Matchar DB, Matsushita K, Mussolino ME, Nasir K, O'Flaherty M, Palaniappan LP, Pandey A, Pandey DK, Reeves MJ, Ritchey MD, Rodriguez CJ, Roth GA, Rosamond WD, Sampson UK, Satou GM, Shah SH, Spartano NL, Tirschwell DL, Tsao CW, Voeks JH, Willey JZ, Wilkins JT, Wu JH, Alger HM, Wong SS, Muntner P (2018) Heart disease and stroke statistics—2018 update: a report from the American Heart Association. Circulation 137(12):67
2. Mirabel M, Iung B, Baron G, Messika-Zeitoun D, Détaint D, Vanoverschelde JL, Butchart EG, Ravaud P, Vahanian A (2007) What are the characteristics of patients with severe, symptomatic, mitral regurgitation who are denied surgery? Eur Heart J 28(11):1358
3. Samad Z, Shaw LK, Phelan M, Glower DD, Ersboll M, Toptine JH, Alexander JH, Kisslo JA, Wang A, Mark DB, Velazquez EJ (2018) Long-term outcomes of mitral regurgitation by type and severity. Am Heart J 203:39
4. Kohorst K, Pretorius M (2018) Future technology of mitral valve repair and replacement for mitral valve disease. In: Seminars in cardiothoracic and vascular anesthesia, vol 23, no 1, p 1
5. Pan M, Jiménez-Quevedo P, Serrador A, Pérez de Prado A, Mesa D, Estévez Loureiro R (2017) Selection of the best of 2016 in MitraClip therapy for the treatment of functional mitral regurgitation. Revista Española de Cardiología (Engl Ed) 70(3):216
6. Cesna S, De Backer O, Søndergaard L (2017) Rapid adoption of transcatheter aortic valve replacement in intermediate- and high-risk patients to treat severe aortic valve stenosis. J Thorac Dis 9(6):1432
7. Van Mieghem NM, Piazza N, Anderson RH, Tzikas A, Nieman K, De Laat LE, McGhie JS, Geleijnse ML, Feldman T, Serruys PW, De Jaegere PP (2010) Anatomy of the mitral valvular complex and its

implications for transcatheter interventions for mitral regurgitation. J Am Coll Cardiol 56(8):617
8. Bateman MG, Iaizzo PA (2012) Imaging in the context of replacement heart valve development: use of the Visible Heart® methodologies. Cardiovasc Diagn Therapy 2(3):220
9. Leopaldi AM, Wrobel K, Speziali G, van Tuijl S, Drasutiene A, Chitwood WR (2018) The dynamic cardiac biosimulator: a method for training physicians in beating-heart mitral valve repair procedures. J Thorac Cardiovasc Surg 155(1):147
10. Taramasso M, Candreva A, Pozzoli A, Guidotti A, Gaemperli O, Nietlispach F, Barthelmes J, Emmert MY, Weber A, Benussi S, Alfieri O, Maisano F (2015) Current challenges in interventional mitral valve treatment. J Thorac Dis 7(9):1536
11. LifeLike BioTissue (2016) LifeLike BioTissue's Mitral Valve. http://lifelikebiotissue.com/shop/cardiac-surgery/mitral-valve. Accessed 3 Oct 2018
12. Mahmood F, Owais K, Taylor C, Montealegre-Gallegos M, Manning W, Matyal R, Khabbaz KR (2015) Three-dimensional printing of mitral valve using echocardiographic data. JACC Cardiovasc Imaging 8(2):226
13. Vukicevic M, Puperi DS, Jane Grande-Allen K, Little SH (2017) 3D printed modeling of the mitral valve for catheter-based structural interventions. Ann Biomed Eng 45(2):508
14. Sardari Nia P, Heuts S, Daemen J, Luyten P, Vainer J, Hoorntje J, Cheriex E, Maessen J (2016) Preoperative planning with three-dimensional reconstruction of patient's anatomy, rapid prototyping and simulation for endoscopic mitral valve repair. Interact Cardiovasc Thorac Surg 24(2):163
15. Grbic S, Easley TF, Mansi T, Bloodworth CH, Pierce EL, Voigt I, Neumann D, Krebs J, Yuh DD, Jensen MO, Comaniciu D, Yoganathan AP (2015) Multi-modal validation framework of mitral valve geometry and functional computational models. In: Statistical atlases and computational models of the heart. Imaging and modelling challenges, vol 8896, p 239
16. Vukicevic M, Mosadegh B, Min JK, Little SH (2017) Cardiac 3D printing and its future directions. JACC Cardiovasc Imaging 10(2):171
17. Ginty OK, Moore JM, Xu Y, Xia W, Fujii S, Bainbridge D, Peters TM, Kiaii BB, Chu MW (2018) Dynamic patient-specific three-dimensional simulation of mitral repair: can we practice mitral repair preoperatively? Innov Technol Tech Cardiothorac Vasc Surg 13(1):11
18. Kikinis R, Pieper SD, Vosburgh KG (2014) 3D slicer: a platform for subject-specific image analysis, visualization, and clinical support. In: Intraoperative imaging and image-guided therapy. Springer, New York, NY, pp 277–289
19. Yoo TS, Ackerman MJ, Lorensen WE, Schroeder W, Chalana V, Aylward S, Metaxas D, Whitaker R (2002) Engineering and algorithm design for an image processing API: a technical report on ITK-the insight toolkit. Stud Health Technol Inform 85:586
20. Scanlan AB, Nguyen AV, Ilina A, Lasso A, Cripe L, Jegatheeswaran A, Silvestro E, McGowan FX, Mascio CE, Fuller S, Spray TL, Cohen MS, Fichtinger G, Jolley MA (2018) Comparison of 3D echocardiogram-derived 3D printed valve models to molded models for simulated repair of pediatric atrioventricular valves. Pediatric Cardiol 39(3):538
21. Caselles V, Kimmel R, Sapiro G (1997) Geodesic active contours. Int J Comput Vis 22(1):61
22. Carnahan P, Ginty O, Moore J, Lasso A, Jolley, M, Herz C, Eskandari M, Bainbridge D, Peters T (2019) Interactive-automatic segmentation and modelling of the mitral valve. In: Springer Lecture Notes in Computer Science, FIMH Proceedings . ArXiv:1905.01344
23. Boone N, Moore J, Ginty O, Bainbridge D, Peters T (2019) A dynamic mitral valve simulator for surgical training and patient specific preoperative planning. In: Medical imaging 2019: image-guided procedures, robotic interventions, and modeling, SPIE Proceedings, vol 10951